Influence of the temperature dependence of anisotropy on the magnetic behavior of nanoparticles

C. de Julián Fernández*
Dipartimento di Fisica, Università di Padova, Via Marzolo 8, I-35131 Padova, Italy
(Received 4 March 2005; revised manuscript received 20 April 2005; published 25 August 2005)

The influence of the temperature dependence of magnetic anisotropy on the superparamagnetic behavior and on the coercivity of nanostructured materials is theoretically investigated in Fe, Co, and Ni. These metals—Fe, Co, and Ni—show a more marked decrease of the magnetocrystalline anisotropy from low to room temperature. The thermal-driven demagnetization process is analyzed using the Arrhenius expression, in which the magnetic barrier is described in terms of the bulk temperature dependence of the magnetocrystalline anisotropy of each material. In the case of cobalt, the effect of considering the second order, K_1, and the fourth order, K_2, magnetocrystalline constants is investigated. The blocking temperatures, T_B, have been calculated for a range of particle volumes, V, and for different measurement times. The temperature dependence of the anisotropy produces that the blocking temperature-to-particle volume is not constant for all sizes and that the relaxation times and the magnetic anisotropies values, calculated from the analysis of the measurement time dependence of the T_B, have no relationship with the theoretical ones. In particular, the calculated relaxation time can be strongly reduced. The analysis of the coercivity was accomplished considering oriented cobalt nanoparticles with uniaxial anisotropy. In the temperature region where the magnetic anisotropy changes, the field dependence of the effective magnetic anisotropy follows a $(1-H/H_{CR})^{\alpha}$ dependence where H_{CR} and α depend on the $K_1(T)$ and $K_2(T)$ values, with being α smaller than 2 (that is, the value obtained with the Stoner-Wohlfarth model). The temperature dependence of the coercive field does not follow the classical $1-(T/T_B)^{\beta}$ expression, or it follows but with the β factor much larger than the 0.5 value. The results are discussed to evidence how the influence of the temperature dependence of the anisotropy or other features of the nanostructured materials influence the interpretation of magnetic measurements.

DOI: 10.1103/PhysRevB.72.054438 PACS number(s): 75.75.+a, 75.30.Gw, 75.60.Jk, 75.20.−g

I. INTRODUCTION

Magnetic nanostructurated materials exhibit novel properties of significant research interest and they are promising materials for applications in medical, microelectronic, spintronic, and magnetic recording technologies. Moreover these materials exhibit magnetic properties which are different from the bulk but also novel—for example enhanced magnetic moment, change of the Curie temperature, enhanced coercivity, exchange coupling effects, nonsaturation effects, giant magnetotransport, and giant Hall effects.[1–4] These effects are associated in complex and interlaced ways with their small-scale length, to dimensionality effects, to the magnetic surface contribution, and to inter- and intraparticle interactions.[3,5–7] However, in general, nanoparticles (forming granular solids, nanopowders, ferrofluids, and dots on surfaces) are considered to be single domain[1,8,9] and their demagnetization process occurs throughout the coherent rotation of all spins of the nanoparticle. The magnetization is oriented in some directions, called easy axes, that correspond to minima on the magnetic energy map. The change of the orientation of the magnetization to other minima is limited by a magnetic barrier that is called magnetic anisotropy. The Stoner-Wohlfarth (S-W) model[8] described this process in an ensemble of noninteracting single-domain particles. That model investigated the magnetostatic reversal process, that is, how the magnetization reverse in presence of the applied field. The effect is to reduce the magnetic barrier between two minima. In the S-W model the magnetic anisotropy depends on the shape anisotropy and on the magnetocrystalline anisotropy of the material. The main conclusion is that the switching field, the necessary field to reverse the magnetization, and the coercive force are proportional to the magnetic anisotropy and inversely proportional to the saturation magnetization.

On the other hand, Bean and Livinston[10] studied the problem of single-domain nanoparticles at thermal equilibrium. Néel[11] proposed that the time, t, necessary to reach the equilibrium depends on the magnetic energy barrier Δ and on the temperature T and can be described by the Arrhenius law

$$t = \tau_0 e^{\Delta/k_B T}, \tag{1}$$

where τ_0 is the characteristic relaxation time and k_B is the Boltzmann constant. Δ corresponds to the total magnetic energy barrier that limits the free rotation of the magnetization maintains this along the anisotropy direction. In a coherent rotation process, the magnetic energy barrier is equal to the product between the particle volume, V, and the magnetic anisotropy, K_{ef}, so that $\Delta = K_{ef}V$. In thermal equilibrium, the magnetic behavior is similar to the atomic paramagnetism and it is therefore called superparamagnetism.[10] At room temperature this effect is dominant in nanostructured materials due to their small sizes: The relaxation time is smaller that the typical measurement time of most of magnetometers.

The blocking temperature, T_B, is the threshold temperature between the blocked regime, where irreversible processes are present, and the superparamagnetic regime. Nanostructured materials are characterized by a blocking temperature distribution. This includes the information about the complex relationship regarding the individual and collective demagnetization processes and the nanostructural features of the material. In many cases it is thought that the demagnetization process can be described in terms of the coherent rotation model in which the ensemble process is represented by a single effective anisotropy. Considering Eq.

(1), the ratio between the blocking temperature and the particle volume is proportional to the magnetic anisotropy

$$\frac{T_B}{V} = \frac{1}{k_B \ln(\tau_m/\tau_0)} K_{ef}, \tag{2}$$

where τ_0 takes values between 10^{-9} and 10^{-11} s (Ref. 12) and τ_m is the time of the experimental measurements. Then the K_{ef} of a nanostructured material can be obtained from magnetometric or susceptibility measurements and from structural studies that give information regarding the blocking temperature distribution and the experimental particle size distribution,[7,13,14] respectively.

Néel[11] and Brown[15] also investigated the effect of random thermal fluctuations as a mechanism of overcoming the magnetic barrier that determines the coercivity. Coercive field and remanent magnetization decrease due to these thermal effects. In this sense, the study of the superparamagnetic behavior is interesting for magnetic recording applications because it constitutes an important limitation to the miniaturisation of magnetic bits.[16,17] Also, the temperature dependence of the coercive field constitutes a complementary measurement to realize this type of study.[18–20]

Most of the magnetic works on nanostructured materials are related to the study of their properties in a wide temperature range, particularly the blocking temperature distribution associated with the particle size distribution. Implicitly it is assumed that the magnetic properties of the materials do not change in all the range of temperatures. However, the change of the magnetic anisotropy with temperature is a known physical property of all magnetic materials and it is expected that this change of magnetic anisotropy must be present, perhaps modified, in nanostructured materials. Only some works[21–24] have been considered the possibility of this effect.

Another interesting point is that the magnetic anisotropy of the nanoparticles is typically represented by a uniaxial single anisotropy and described by a single effective anisotropy. But there are several current studies that indicate that the possibility of an incoherent reversal process is presented.[3,25] Also, Wernsdorfer and colleagues have shown in several studies[26–31] that the angular dependence of the magnetic barrier of a single nanoparticle cannot be simply described by a uniaxial anisotropy with a single anisotropy constant. So it appears interesting to investigate the consequence of considering a complex description of the anisotropy in the properties of nanostructured materials.

The purpose of this work is to show how the change of the magnetic anisotropy with temperature gives rise to different features of the superparamagnetism behavior with respect to those expected in the "a-thermal" classical model. We will analyze the relationship between the blocking temperature and the size of nanoparticles with different temperature dependences of the anisotropy using the corresponding values of the Fe, Co, and Ni metals. The fourth-order magnetocrystalline cubic constant, K_{1C}, of Ni decreases more than one order of magnitude from low temperature to room temperature, while the variation for Fe is very small. Cobalt is an intermediate case. Also, these materials exhibit different magnetocrystalline structure: Ni and Fe have cubic anisotropy but with $K_{1C}<0$ and $K_{1C}>0$, respectively, while for Co the anisotropy is uniaxial. The case of cobalt will be deeply investigated because uniaxial anisotropy is used for the description of the anisotropy in nanostructured materials. We have compared the superparamagnetic behavior and the temperature dependence of the coercive field when the angular dependence of the barrier is described only by the K_1 term or by K_1 and the fourth-order anisotropy term, K_2 (with the respective temperature dependence). In Co, this last term is not negligible at low temperatures.

This work is organized in the following way: We will present in the next section the analytical expressions that are considered to describe the superparamagnetic behavior and the coercivity of the nanoparticles. The third part will show the results regarding superparamagnetic behavior, that is, the analysis of the relationship between the T_B and particle volume considering (i) one constant measurement time, and (ii) different measurement times. Also the expressions regarding the temperature dependences of the coercive field of oriented cobalt nanoparticles are shown. Finally a discussion of the results is presented.

II. THEORETICAL

In the S-W model, K_{ef} depends on the magnetocrystalline shape and magnetoelastic anisotropies. In this work we will only consider the magnetocrystalline anisotropy. Iron and nickel have cubic magnetic anisotropy and the angular dependence of the magnetic anisotropy is described by

$$E_K(\alpha_1, \alpha_2, \alpha_3, T) = K_{1C}(T)(\alpha_1\alpha_2 + \alpha_1\alpha_3 + \alpha_2\alpha_3),$$

where α_1, α_1, and α_3 are the cosines of the angles formed between the magnetization and the three main axes, and K_{1C} is the fourth-order cubic anisotropy constant. K_{ef} corresponds to the minimum energy barrier that is found between the two easy axes directions, being[1,32]

$$K_{ef}(T) = \begin{cases} \frac{1}{4} \cdot K_{1C}(T) & \text{if } K_{1C} > 0 \text{(Fe case)} \\ \frac{1}{12} \cdot K_{1C}(T) & \text{if } K_{1C} < 0 \text{(Ni case)}. \end{cases} \tag{3}$$

In the cobalt case, the anisotropy is uniaxial and the angular dependence of the anisotropy is described by

$$E_K(\theta, T) = K_1 \sin^2\theta + K_2 \sin^4\theta, \tag{4}$$

with θ being the angle between the magnetization and the easy axis, and K_1 and K_2 are the second- and fourth-order uniaxial anisotropy constants, respectively. In Eq. (4), if $K_1 > 0$ and $K_2 > 0$, E_K describes the classical uniaxial anisotropy with an easy axis and the barrier between the two easy axis directions, K_{ef}. This takes a different value depending on the anisotropy terms that are taken into account

$$K_{ef}(T) = \begin{cases} K_1(T) \text{ considering only } K_1, \text{ and} \\ K_1(T) + K_2(T) \text{ considering } K_1 \text{ and } K_2. \end{cases} \tag{5}$$

A. Superparamagnetic behavior

In these calculations we have used the temperature dependence of the anisotropy (TDMA) constants of the Fe, Ni, and

Co bulk metals. Combining these data and using the respective relationships between the anisotropy constants and K_{ef}, the blocking temperature is obtained by resolving the redefined Eq. (2)

$$\frac{T_B}{V} = \frac{K_{ef}(T_B)}{k_B \ln(\tau_m/\tau_0)}. \quad (6)$$

From this equation we have calculated:

1. The particle size dependence of the blocking temperature, T_B^{ZFC}, considering a constant value of τ_m. This procedure simulates zero-field-cooled (ZFC) measurements without taking into account the particle size distribution. For these calculations we have chosen $\ln(\tau_m/\tau_0)=25$, which is a typical value used in the magnetometric measurements.

2. The particle size dependence of the blocking temperature, T_B^{sus}, as function of different τ_m. For a particle volume, different (τ_m, T_B^{sus}) couples are represented using the Arrhenius plot:

$$\ln(\tau_m) = A + B\frac{V}{k_B T_B^{sus}}, \quad (7)$$

where A and B are parameters that are obtained from the experimental data. From these, the time τ_0^{sus} and the magnetic anisotropy K_{ef}^{sus} values are calculated by:

$$\tau_0^{sus} = e^A \text{ and} \quad (8)$$

$$K_{ef}^{sus} = B. \quad (9)$$

In this procedure the time scale was varied between 10^2 s and 10^{-5} s, covering in this way the characteristic τ_m of classical ac-susceptibility measurements.

B. Temperature dependence of the coercive field

The temperature dependence of the coercive field, $H_C(T)$, will be investigated for oriented particles with uniaxial anisotropy. The magnetization is placed in the easy axis and the magnetic field is oriented in the opposite direction. Then the starting point is the analysis of the angular dependence of the density of magnetic energy, E_{HK}, described by

$$E_{HK}(H,\theta,T) = -\mu_0 M_S H \cos\theta + K_1(T)\sin^2(\theta) + K_2(T)\sin^4(\theta), \quad (10)$$

where μ_0 is the vacuum permeability constant (for simplicity this term will not be included in the rest of the manuscript), H is the applied field, and M_S is the magnetization saturation. The magnetic barrier is the difference of energy between the energy corresponding to the magnetization in the easy axis and the maximum of the energy calculated from Eq. (10),

$$K_{ef}(H,T) = E_{HT}(H,\theta_{MAX}(H,T),T) - E_{HT}(H,0,T), \quad (11)$$

where θ_{MAX} is the angle for which E_{HT} is maximum for a magnetic field H. The effect of the increase of the applied field is to reduce K_{ef} and, for the critical field, H_{CR}, K_{ef} becomes zero, so the magnetization reverses to the direction of the magnetic field.

In a first case, if K_1 is only considered, the magnetic-field dependence of K_{ef} is analytically calculated, being

$$K_{ef}(H) = K_{ef}(H=0)\left(1 - \frac{H}{H_{CR}}\right)^{\alpha}, \quad (12)$$

where K_{ef} $(H=0)$ is the value of the barrier at zero field and is equal to K_1, $H_{CR}=2K_1/M_S$, and α is 2. In the selected oriented case, the critical field is equivalent to the coercive field and it is equal to the anisotropy field, $H_A=2K_1/M_S$.

If thermal demagnetization effects are considered, the reversal process occurs when

$$K_{ef}[H_{CR}(T_B^{H_C})]V = \ln(\tau_m/\tau_0)k_B T_B^{H_C}, \quad (13)$$

where $T_B^{H_C}$ is the blocking temperature measured from hysteresis loops—that is, the temperature at which the magnetization curves show neither coercivity nor remanent magnetization. The solution of this equation is

$$H_{CR}(T) = H_{CR}(T=0)\left[1 - \left(\frac{T}{T_B^{H_C}}\right)^{\beta}\right], \quad (14)$$

where $H_{CR}(T=0)=H_A$ at 0 K and β is 1/2.

We point out that even if the characteristic times of the ZFC measurements and the $H_C(T)$ measurements are different (depending the apparatus setup, from 1 to 15 hours) their $\ln(\tau_m/\tau_0)$ terms are similar, then typically is considered $T_B^{ZFC} \approx T_B^{HC}$. This indicates that both measurements give similar information about the magnetic properties of a material.

Now we will consider the effect of including K_2. If $K_1/K_2 > 0$, and in absence of thermal-driven effects,

$$K_{ef} = K_1 + K_2,$$

but

$$H_{CR}(0) = 2\frac{K_1}{M_S}. \quad (15)$$

We observe that the magnetic barrier depends on the K_2 value while this does not contribute to the critical field. In the case of taking into account only the K_1 constant, the H_{CR} is equal to H_A, but when K_2 is considered, H_A is $2(K_1+2K_2)/M_S$,[38] so $H_{CR} < H_A$. In the case of randomly oriented particles, H_{CR} depends on K_1/K_2 ratio and their signs.[33,34]

Finally, if the effect of temperature is included, $K_{ef}(H,T)$ and $H_{CR}(T)$ are calculated numerically by resolving Eqs. (11) and (13).

Regarding the coercive field of a material composed of these nanoparticles described only by the K_1 term, it depends on the orientation degree being $H_C=H_{CR}$ if they are oriented, as above described, or $H_C=0.5H_{CR}$ if they are randomly oriented. If K_2 has to be taken into account, the factor between H_C and H_{CR} depends on the K_1 and K_2 values.[34]

III. RESULTS

As previously discussed, the anisotropies of Ni, Fe, and Co are very different, not only because they are different types but also because their anisotropies vary by a different percentage with the temperature. Figure 1(a) represents the temperature variation of the K_{1C} constants[35,36] for the nickel and iron cases, while in Fig. 1(b), $K_1(T)$, $K_2(T)$, and $K_1(T)$

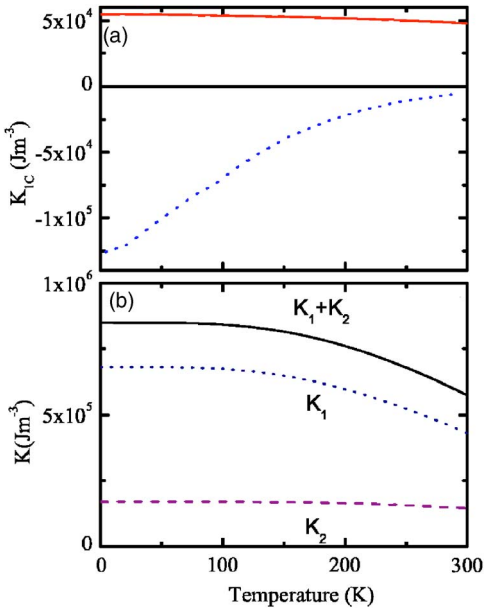

FIG. 1. (Color online) (a) The temperature variation of the K_{1C} constant for nickel[35] (dotted line) and iron[37] (solid line); (b) The temperature variation of the K_1 (dotted line), K_2 (dashed line) and K_1+K_2 (solid line) constants for cobalt.[35]

$+K_2(T)$ values for cobalt[36,37] are reported. In Ni, K_{1C} increases almost 22 times from room to low temperature while the change in Fe is only 13%. An intermediate case is the Co, for which K_1 increases 60% from room temperature to 4 K, and including the $K_2(T)$, the K_1+K_2 increases 50%. In all the cases we have considered that $\tau_0=10^{-9}$ s.

A. Blocking temperature versus particle volume

1. $T_B(V)$ with τ_m constant

Figure 2(a) represents the variation of T_B as a function of the particle volume for the Ni and Fe cases, calculated using Eq. (6). The upper part of the abscissa represents the equivalent diameter, $D_{eq}=(6V/\pi)^{1/3}$, that corresponds to each volume.

In the nickel case, the T_B never reaches the room temperature value, which implies that, considering only the magnetocrystalline anisotropy, single-domain nickel nanoparticles are theoretically always superparamagnetic at this temperature. In the a-thermal model, represented by Eq. (2), there is a linear relationship between T_B and V. However taking into account the TDMA, this is not observed in all temperature ranges, showing $T_B(V)$ a trend towards saturation for large volumes. In the a-thermal model, large volumes correspond to large T_B, but if the magnetic anisotropy decreases with the increasing of the temperature, then the T_B will be poorly dependent on the particle volume, as observed in Fig. 2(a) for Ni.

In the case of Fe, the T_B is approximately proportional to V up to a T_B of room temperature because its anisotropy changes little with temperature. Considering these data, the critical volume below which Fe single nanoparticles are superparamagnetic at room temperature is 8.7×10^3 nm^3(D_{eq} =25 nm).

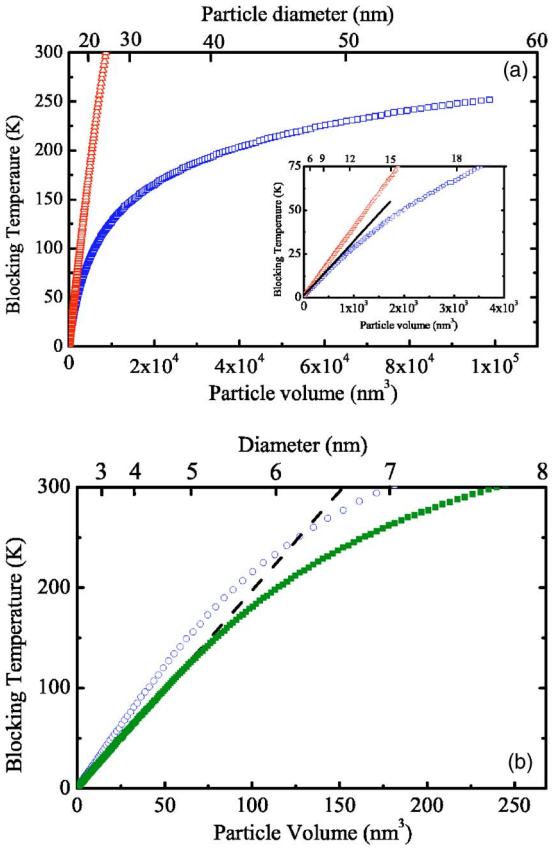

FIG. 2. (Color online) (a) The variation of T_B as a function of the particle volume for the Ni (□) and Fe (△) cases. Inset: detail of the figure for particle volumes smaller than 4×10^3 nm^3. The line helps to illustrate the linear dependence of T_B on particle volume considering that the K_1 is constant with the temperature. (b) The variation of T_B as a function of the particle volume for cobalt considering that the $K_{ef}(T)=K_1(T)$ (■) and that the $K_{ef}(T)=K_1(T)+K_2(T)$ (○). The line represents the variation of the T_B as function of the particle volume calculated using Eq. (2) and considering the K_1 value at 4 K. In the upper abscissas, the equivalent diameters, $D_{eq}=(6V/\pi)$, that corresponds to each volume are represented.

The inset of Fig. 2(a) corresponds to a zoom of this figure in a smaller particle region. In this region, the T_B/V relationship is linear for Ni particle volumes smaller than 10^3 nm^3 (D_{eq}=13 nm) with a $T_B<30$ K. Considering Eq. (3), the calculated $K_{1C}{}'$ is equal to 1.19×10^5 J m^{-3}, which is slightly smaller than the right value at 4 K, 1.25×10^5 J m^{-3}. We point out that if this result will be compared with the magnetic anisotropy at room temperature (5.5×10^3 J m^{-3}), one would arrive at the erroneous conclusion that there is an enhancement of the anisotropy (20 times!). For the Fe case, the T_B vs V shows a linear dependence below 200 K (in the chosen scale), with $K_{1C}{}'=5.27\times10^4$ J m^{-3}, which is also slightly smaller than the exact low temperature K_1 (5.48×10^4 J m^{-3}). In this case the difference between these values and the value at room temperature (4.8×10^4 J m^{-3}) is much smaller than in the nickel case.

Figure 2(b) represents the results obtained in the cobalt case considering that K_{ef} depends on $K_1(T)$ and on the $K_1(T)+K_2(T)$. The T_B/V is not linear above volumes larger than approximately 66 nm^3(D_{eq}=5 nm) and approximately

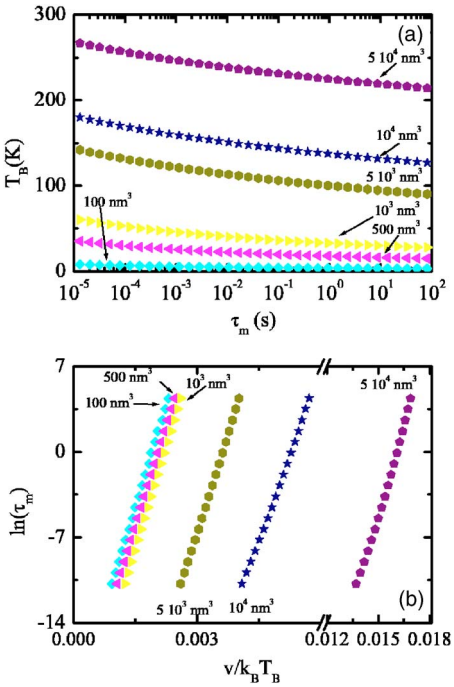

FIG. 3. (Color online) (a) The variation of T_B as a function of the measurement time for different nickel particle volumes; (b) natural logarithm of the measurement times versus V/k_BT_B for different particle volume.

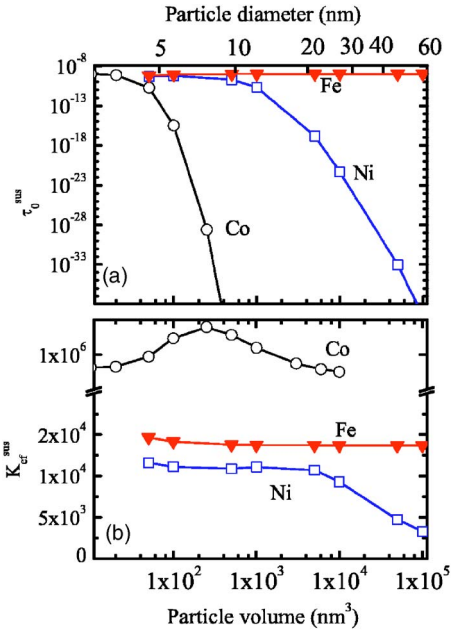

FIG. 4. (Color online) (a) τ_0^{sus} and (b) K_{ef}^{sus} versus particle volume, calculated from Eq. (8) and (9), respectively, for Fe (▼), Ni (□) and Co (○) cases. Continuous lines help to follow the dependences. In the upper abscissa, the equivalent diameter, $D_{eq}=(6V/\pi)$, of each volume is represented.

45 nm^3(D_{eq}=4.4 nm), if $K_1(T)$ and $K_1(T)+K_2(T)$ values are respectively used. The contribution of $K_2(T)$ increases the T_B/V rate with respect to the values obtained, considering only K_1 due to the larger effective anisotropy of K_1+K_2. In this figure, it has also been illustrated with a dashed line the theoretical dependence of T_B/V in the approximation of using only K_1 at 4 K. This value and the value at room temperature are often considered when discussing the magnetic behavior of cobalt nanostructures. Below 130 K the straight line obtained with this approximation coincides with the curve calculated using only $K_1(T)$. As can be observed in Fig. 1, above this temperature the K_1 begins to decrease as temperature increases. However, this approximation has not taken into account the K_2 contribution to the total anisotropy. This approximation underestimates the real value of the blocking temperature in nanoparticles with a T_B below 255 K. For nanoparticles with a larger T_B, this approximation overestimates their blocking temperature because it does not take into account the decreasing anisotropy as temperature increases.

2. $T_B(V)$ as function of τ_m

Figure 3(a) represents the dependence of the T_B^{sus} of the measurement time for the Ni case considering nanoparticles with volumes from 5×10^4 nm^3(D_{eq}=46 nm) to 100 nm^3(D_{eq}=6 nm). The T_B^{sus} of nanoparticles with volume smaller than 100 nm^3 depends poorly on the time measurement, and the corresponding curves have not been represented. The represented results accord qualitatively with the expected behavior reflected by Eq. (2) and (7): the T_B^{sus} is larger as the particle size is larger and it decreases as τ_m increases. However, this decreasing is stronger in the larger particles than in the smaller ones. The effects of considering the TDMA are better evidenced analyzing the data with the Arrhenius plot, as is shown in Fig. 3(b). In the selected scale, for volumes smaller than 10^4 nm^3 (D_{eq}=27 nm), the $\ln(\tau_m)$ presents the classical linear dependence of $V/k_BT_B^{sus}$ while for larger volumes it can be observed that the relationship between both terms is not linear. The curves of all the volumes do not super impose, opposite as expected, nor do they have the same zero, indicating that for each particle volume different τ_0^{sus} and K_{ef}^{sus} are obtained. In the case of Fe and Co, the K_B^{sus} and τ_m^{sus} curves show similar features than in the Ni case, with $\ln(\tau_m)$ almost linearly dependent of $V/k_BT_B^{sus}$ for all the considered volume range.

Figure 4(a) represents the τ_0^{sus} values for the Fe, Ni, and Co cases, which have been calculated for volumes that have a T_B^{sus} smaller than 300 K in all the τ_m range. The Co case was calculated considering K_1 and K_2 anisotropies. For Fe, the τ_0^{sus} of the smallest volumes are slightly smaller than $\tau_0=10^{-9}$ s, originally included in Eq. (6) and they approach this value as volume increases. These τ_0^{sus} values are almost independent of the particle volume in comparison with those obtained in the Ni and Co cases. In these latter cases, volume dependence of τ_0^{sus} shows two regimes: For the smallest volumes, the τ_0^{sus} are slightly smaller than τ_0, and for the largest sizes the τ_0^{sus} decreases. In this second regime, over a certain volume, τ_0^{sus} drops to much smaller values than 10^{-9} s. The critical volumes for Ni and Co, above which the second regime begins, are 10^3 nm^3 (D_{eq}=12.5 nm) and 200 nm^3 (D_{eq}=7 nm), respectively. In both cases the comparison of the temperature dependence of K_1, $\ln(\tau_m)$ vs $V/k_BT_B^{sus}$ and $\tau_0^{sus}(V)$ indicates that for this critical volume the corresponding blocking temperature range coincides with the tempera-

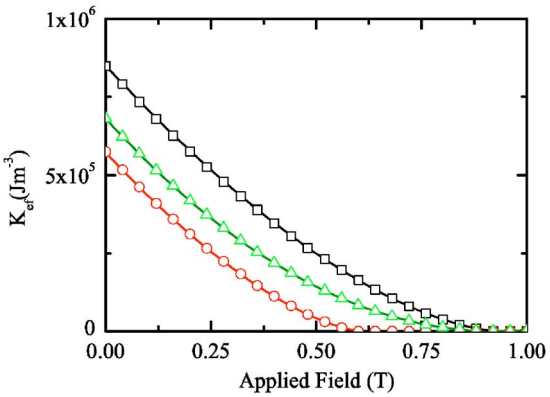

FIG. 5. (Color online) Dependence of the effective magnetic anisotropy of the applied field for cobalt calculated using Eq. (10) and considering only K_1 term with the value at 4 K (△) and the K_1 and K_2 terms with the values at 4 K (□) and 300 K (○). Lines correspond to the fit of the data to Eq. (12).

ture range at which the magnetic anisotropy begins to decrease. We observe that the τ_0^{sus} values obtained in this second regime have no physical sense.

Regarding the volume dependence of K_{ef}^{sus}, represented in Fig. 4(b), Fe, Ni, and Co have different behaviors. The K_{ef}^{sus} of Fe is almost independent of the particle size; for Co a maximum for the volume of 250 nm^3 (D_{eq}=8 nm) is observed and for the Ni case, there is a large decrease in the K_{ef}^{sus} from volumes larger than 5×10^3 nm^3 (D_{eq}=21 nm). It is interesting to compare K_{ef}^{sus} with the corresponding K_{1C}, K_1, and K_2, taking into account Eqs. (3) and (5). We observe that for Fe, $K_{ef}^{sus}/4=1.37-1.2\times10^4$ J m^{-3} (maximum and minimum values) are slightly smaller than K_{1C}, $1.47-1.4\times10^4$ J m^{-3}, values at low and room temperature, respectively, while the differences are larger for Ni and Co. In the case of cobalt, the maximum value of K_{ef}^{sus} (13.5×10^5 J m^{-3}) is much larger than any value of K_1+K_2 which could be eventually analyzed as an enhancement of the magnetic anisotropy.

B. Temperature dependence of the coercivity of cobalt nanoparticles

1. Field dependence of the magnetic barrier

We have investigated the influence of the second- and fourth-order anisotropy constants in the field dependence of the effective barrier $K_{ef}(H)$ considering that in the density of the magnetic energy [Eq. (10)], (i) the term K_1 with value at the temperature of 4 K is only considered and including the K_1 and K_2 terms with respective values at the temperatures of (ii) 4 K and (iii) of 300 K. The results are represented in Fig. 5. In case (i), excellent agreement is obtained with Eq. (12), with α=2 and H_{CR}=0.923 T. This last value is exactly $2K_1(T=4\text{ K})/M_S$, so we reproduce the expected α and H_{CR} values of the S-W model. For cases (ii) and (iii), the respective $K_{ef}(H)$ also reproduce Eq. (12) with $K_{ef}(0)$ values similar to K_1+K_2; however, the α are different than in case (i), being 1.6 and 1.523 respectively. The H_{CR} are 0.933 T and 0608 T for (ii) and (iii) cases, slightly larger than the respective $2K_1/M_S$, 0.923 T and 0.586 T. These results confirm the validity of Eq. (12) to calculate the $K_{ef}(H)$ but including α and H_{CR} factors that depend on the $K_1(T)$ and $K_2(T)$ values.

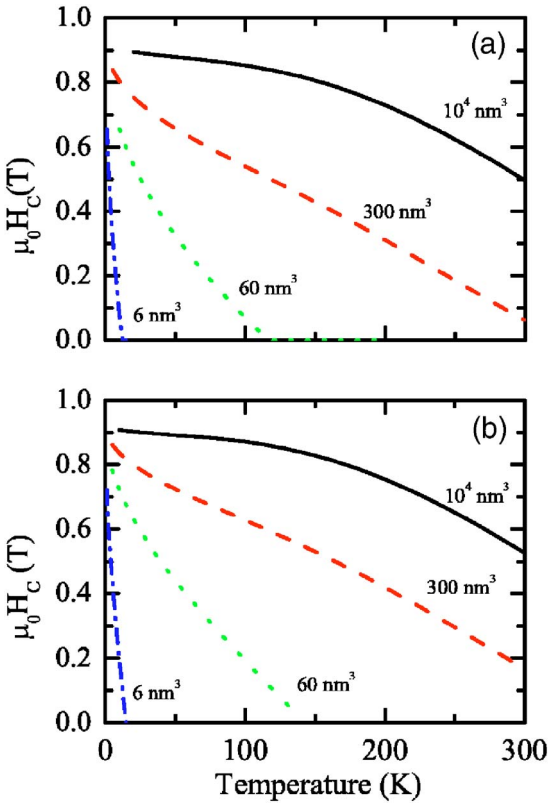

FIG. 6. (Color online) Temperature dependence of the coercive field for different particle volumes calculated considering (a) only the $K_1(T)$ term and (b) the $K_1(T)$ and $K_2(T)$ terms.

2. Temperature dependence of the critical field

Next, the temperature dependence of H_{CR} for different particle volumes was calculated resolving Eq. (13) and considering two different cases: (i) $K_{ef}(T)=K_1(T)$ and (ii) $K_{ef}(T)=K_1(T)+K_2(T)$. In Figs. 6(a) and 6(b) the corresponding results are represented. In both cases the $H_{CR}(T)$ show a continuous decreasing of the critical field and a blocking temperature $T_B^{H_C}$ as is commonly expected.

We observe that the shapes of the curves change depending on the considered particle volume and also, for a determined volume, on the terms considered in the definition of anisotropy. The analysis of the curves, considering Eq. (14), supports these observations. In cases (i) and (ii), the shape of the $H_C(T)$ curves cannot be fitted in all the temperature ranges in Eq. (14). For larger volumes, the shape of the curves is concave decreasing, which means that the coercive field decreases much faster as temperature increases ($\partial H_{CR}/\partial T>1$). For smaller volumes, the shape of the curve is convex decreasing ($\partial H_{CR}/\partial T<1$), indicating that the magnetic behavior of these materials is different. A volume of 300 nm^3 (D_{eq}=8 nm) appears as an intermediate case. For volumes smaller than 300 nm^3 and below 100 K, $H_C(T)$ reproduces Eq. (15) in cases (i) and (ii). However the $H_{CR}(0)$ and β factors, reported in Table I, are quite different than the

TABLE I. $H_{CR}(0)$, T_B^{HC} and β calculated from Eq. (15) as a function of different particle volumes and considering the $K_{ef}=K_1(T)$ and $K_1(T)+K_2(T)$. T_B^{ZFC} corresponds to the values obtained from Eq. (10)

V (nm)	$K_{ef}=K_1(T)$			$K_{ef}=K_1(T)+K_2(T)$			
	$H_{CR}(0)$	T_B^{HC}	β	$H_{CR}(0)$	T_B^{HC}	β	T_B^{ZFC}
6	0.923	11.8	0.50	0.88	14.9	0.63	16
60	0.900	116	0.52	0.86	144	0.67	143
300	0.818	332	0.92	0.82	362	1.15	367
10^4	0.889	432	2.21	0.93	492	1.70	551

theoretical $2K_1/M_S$ and 0.5. The factor β is much larger than 0.5, indicating a strong variation of the $H_C(T)$ as expected. For volumes smaller than 300 nm^3 and $T_B<100$ K, $H_C(T)$ also follows Eq. (14) and results are included in Table I. In case (i), as can be observed in Table I, $H_{CR}(0)$ and β values are similar to the corresponding classical values, while for case (ii) these are smaller and larger, respectively. The larger value of β in case (ii) can be understood, considering that $\beta\approx 1/\alpha$ and that $\alpha<2$ when K_2 is included. Also in this case we conclude that the $H_{CR}(0)$ is systematically smaller than the expected ones. Finally it can be observed in Table I that, except for the larger volumes, the T_B^{HC} obtained with the fit using K_1 and K_2 are in good agreement with the T_B^{ZFC}.

IV. DISCUSSION

The presented results show how taking into account the temperature dependence of the anisotropy gives rise to a phenomenology of the superparamagnetism different than is commonly considered. One first point to discuss is if it is reasonable that the TDMA exists and why can it be important in nanostructured materials whose properties are determined by size effects. The Curie temperature, T_C, of Fe, Ni, and Co is well above the temperature range at which we have done our calculations. It is known that, in these materials, near the T_C, the magnetic anisotropy decreases following a T^δ law, where $\delta=7$ to 10, according to the pair model of the anisotropy.[38,39] In the case of Co, this decreasing is observed even at lower temperatures due to this metal showing the hcp-fcc transition at 698 K, which modifies its magnetic properties. In fact, if an order temperature is near or below room temperature, the change with the temperature of the magnetic anisotropy must be taken into account in order to analyze its magnetic features.[40] Ferromagnetic or spin-frustrated antiferromagnetic nanostructurated materials[5,25,41,42] have low Curie or Néel temperature and so directly fulfil this condition. Therefore, core-shell nanostructures composed totally or partially of oxides show these phenomena. This must also occur in metallic nanoparticles where the anisotropy is determined by the surface contribution.[1,6,7,43] We deduce this considering that it is well known that the Curie temperature of the surface of magnetic thin films[44] is smaller than that of bulk ones due to the reduced coordination of the surface atoms. Similar behavior is expected in the surface of nanoparticles. In addition, we observe that nanoparticles show reduced T_C due to size effects,[2] which produces an enhancement of the thermal demagnetization. Considering these arguments, we conclude that is reasonable to think that the magnetic anisotropy of nanoparticles should change with the temperature and its temperature variation could depend on size.

In many studies of the magnetic properties of nanoparticulated materials, the ZFC-FC (field-cooled) measurements are analyzed considering that the blocking temperature distribution depends only on the particle-size distribution and that the anisotropy is constant in all the range of temperatures in which the measurements were done. Considering a hypothetical size distribution, the corresponding calculated blocking-temperature distributions are different if it is assumed that the anisotropy is constant with the temperature or it decreases with the increasing of the temperature. In order to illustrate this aspect, we have simulated the ZFC-FC magnetizations of an ensemble of cobalt nanoparticles with a size distribution that has the corresponding T_B distribution in a temperature region where the anisotropy changes. The ZFC magnetizations are calculated using the expression[13,14]

$$M_{ZFC}(T)=M_S\int_0^{V_B(T)}L(x)Vf(V)dV+\frac{M_S^2H}{3K_{ef}}\int_{V_B(T)}^{\infty}Vf(V)dV, \tag{16}$$

where $L(x)$ is the Langevin function, $x=M_SHV/k_BT$, $f(V)$ is the particle size distribution, and $V_B(T)$ is the threshold blocking volume at the temperature T between the blocked and the superparamagnetic regimes. The FC magnetizations are calculated using the expressions

$$M_{FC}(T)=M_S\int_0^{V_B(T)}L(x)Vf(V)dV+M_S\int_{V_B(T)}^{\infty}L(x_B)V_Bf(V)dV, \tag{17}$$

where x_B is the value of x for V_B.

In both expressions the first part corresponds to the superparamagnetic contribution while the second part corresponds to the magnetization of the blocked nanoparticles. If we consider that the anisotropy changes with temperature, $V_B(T)$ must be calculated with Eq. (6), while if the anisotropy is constant we use Eq. (2). Figure 7 represents the ZFC-FC magnetizations calculated, considering that the $K_{ef}(T)$ depends on both $K_1(T)$ and $K_2(T)$ [Eq. (5)] for a log-normal particle-size distribution[45] with an average diameter of $D_m=5$ nm and as $\ln(\sigma)=0.15$ and taking $M_S=1.92$

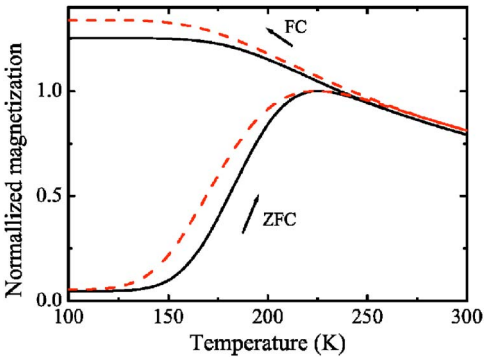

FIG. 7. (Color online) Temperature dependence of the ZFC and FC magnetizations corresponding to a ensemble of cobalt nanoparticles characterized by a particle log-normal distribution and considering that K_{ef} changes with temperature (—) (considering $K_1(T)$ and $K_2(T)$) and that it is constant and equal to 7.45×10^5 J m^{-3} (---).

$\times10^6$ A m^{-1}. Also included in this figure are the ZFC-FC magnetization calculations regarding the constant value of $K_{ef}=7.45\times10^5$ J m^{-3}. With this value, we obtain a ZFC curve whose maximum, T_{max}, is at the same temperature as the calculated curves taking into account the TDMA. Both types of ZFC-FC curves, calculated with the approximation of constant anisotropy and with $K_{ef}(T)$, have been normalized to make the positions of the maximum of the ZFC curves coincide in order to demonstrate their differences. As can be observed, ZFC-FC magnetization curves corresponding to $K_{ef}(T)$ are more narrow than the curves obtained when the anisotropy is constant. This indicates that the real blocking temperature distribution is narrower than that which would be calculated using a constant anisotropy. This is because, if we consider the volume that corresponds to T_{max}, for volumes smaller or larger, the anisotropy is larger and smaller, respectively; so the number of particles with the T_B near T_{max} is larger than the case of considering K_{ef} constant for all volumes. Taking into account this aspect, we observe that the temperature at which ZFC and FC curves join is larger considering K_{ef} constant than $K_{ef}(T)$. In a first instance, this could means that the choice of constant K_{ef} give rise to an apparent enhancement of the anisotropy. Also a simple calculation, quite often used, of the average K_{ef} from Eq. (2), using the T_{max} and the average particle size calculated with respect to the experimental particle distribution (in the log-normal distribution, $V_m=\pi/6D_m^3e^{9(\ln^2\sigma)}=8\times10^{-26}$ m^3, gives $K_{ef}=9.8\times10^5$/J m^{-3}. This value is larger than the real effective anisotropy of the cobalt $K_1+K_2(T_{max}=217\text{ K})=7.4\times10^5$ J m^{-3}. In conclusion, the analysis of ZFC-FC data, assuming that the magnetic anisotropy is constant in a temperature range where it is really decreasing, produced an apparent enlargement of the blocking temperature distribution and also an apparent enhancement of the calculated effective anisotropy.

The second conclusion of our results is related to the measurement time dependence of the T_B: If the deblocking process occurs in a temperature range where the anisotropy varies, the Arrhenius plots give τ_0^{sus} and K_{ef}^{sus} values that are not related to the real properties of the nanoparticles. While this fact is expected in the interpretation of the meaning of K_{ef}^{sus}, because K_1 changes with temperature, that is not the case for τ_0^{sus} because τ_0 is constant in our approximation. In our calculations, we have considered that the relaxation time is 10^{-9} s while, if the anisotropy decreases in the temperature interval where the measurements are done, the calculated τ_0 value could be several orders of magnitude smaller. A large number of experimental studies[46–50] have obtained τ_0 with values much smaller than those considered for the reversal process (10^{-8}–10^{-10} s). The physical mechanism that produces this effect is the subject of controversial discussion and it is typically interpreted in terms of the frustration effects or spin-glass effect due to the competition of interparticle interactions and/or the uncompensated antiferromagnetic order in the surface or in the core of nanoparticles.[1,41,42,46,47,51–54] We show here how the temperature dependence of the anisotropy in the nanoparticles can give rise to similar results. This effect could be understood simply by considering the magnetic behavior above the temperature, T_0, over which K_{ef} begins to change. In a first approach this change can be approximated by the linear expansion of $K_{ef}(T)$ by $K_{ef}(T_0)+T\cdot\partial K(T_0)/\partial T$. The equivalent Eq. (1) and Eqs. (2) and (6) are transformed in

$$\ln(\tau_m)=\ln(\tau')+\frac{K_{ef}V}{k_BT}, \tag{18}$$

where

$$\tau'=\tau_0e^{\partial K_{ef}/\partial T|_{T_0}V/k_B},$$

τ' is τ_0^{sus}. This term depends on the temperature and it varies exponentially with V and with $\partial K(T_0)/\partial T$. For Co and Ni, $|\partial K(T_0)/\partial T|$ is larger for larger volumes due to the large corresponding T_B, so the exponential factor is doubly increased. We observe that $\partial K(T_0)/\partial T$ is negative as temperature increases, so τ_0^{sus} is smaller in comparison to τ_0.

Regarding the effect on the temperature dependence of the coercive field, we point out that their shapes, concave or convex, and the calculated β and the $H_C(0)$ values change with respect to the values of the S-W model. In particular, we find that β is larger than 1. Classically, as said, $\beta=0.5$ and increases to 0.77 if nanoparticles are randomly oriented. Values different from these have been observed by Bonacchi *et al.*[55] in NiO nanoparticles and by Tronc[22,23] in γ oxide nanoparticles. We observe that in both cases they are materials with a reduced T_C. In order to adequately confirm our calculations with experiments, it will be required to develop our calculations in the case of randomly oriented nanoparticles. At the same time experimental results must be analyzed separating the blocking and superparamagnetic contributions.[56,57]

From the experimental point of view, it will be difficult to observe the changes of the anisotropy with temperature, because the effective anisotropy includes many contributions—surface, shape, and interparticle interactions—and their different temperature dependences. Considering also that in a material there is a distribution of nanostructural features (shape, size, surface, concentration) and, considering the narrow relationships between magnetic and structural features, then the magnetic anisotropy is defined by a distribution of

barriers in which can be difficult to identify changes in temperature. Only recently has it been possible to characterize one single nanoparticle (see Wernsdorfer and colleagues).[20,28,29,31] Unfortunately, the temperature range at which these measurements are done is short and it is made at very low temperatures, so one cannot observe the effects proposed in this work. The studies of this group are mainly related to the study of the angular dependence of the switching field of single fcc Co nanoparticles. They observed that the magnetic barrier is described with a more complex expression than Eq. (10), including cubic and uniaxial terms. So the interest of investigating the contribution of K_2 in the definition of the magnetic anisotropy is not only to do a more complete definition of the anisotropy for cobalt but also to investigate a closer description of the barrier to the characteristic of nanostructured materials. The first simple conclusion when considering K_2 in the analysis of the barrier is that the blocking temperature and the coercive field must increase. We have shown that in oriented nanoparticles this is true for the blocking temperature but not for the coercivity. As shown in Eq. (15), the coercive field depends only on K_1 and not on K_2. The K_{ef} calculated from the coercive field, using Eq. (15), will give rise to smaller K_{ef} than those obtained from ZFC measurements obtained by resolving Eq. (6). The main contribution of K_2 is to modify the field dependence of the magnetic barrier $\Delta E(H)$, giving rise to an α exponent smaller that 2 and producing a temperature dependence of the coercive field with a β exponent different from 0.5. This behavior depends on the temperature dependence of both K_1 and K_2.

Regarding the limits of our model, it is clear that we have not assumed any surface anisotropy, shape anisotropy, interparticle coupling, etc. because we consider that the reversal process occurs by coherent rotation of the single domain. However, within the S-W framework, the coherent rotation is energetically more stable than incoherent rotation modes or multidomain only if the particle size is smaller than the critical single-domain diameter, D_{cr}.[3,58] This size then defines a size limit for the S-W model and for our considerations. We consider the expression $D_{cr}=5.1\times(A_{exch}/\mu_0 M_S^2)^{1/2}$ (Ref. 58), where A_{exch} is the exchange stiffness. Taking A_{exch} equal to 2.5×10^{-11} J/m,[59] 1.3×10^{-11} J/m (Ref. 60) and 0.8×10^{-11} J/m (Refs. 61 and 62) for bulk Fe, Co, and Ni, the corresponding D_{cr} are 26 nm (volume$=9.4\times10^3$ nm^3), 23 nm (6.1×10^3 nm^3) and 50.5 nm (67.5×10^3 nm^3). In the case of Ni and Fe, our calculations were realized for particle diameters above the respective D_{cr}, so incoherent rotation modes or two-wall formation cannot be ruled out. In this study we have considered that the only property that changes with temperature is the magnetic anisotropy. However, for example, the magnetization saturation changes with temperature. This is particularly important for nickel, which has a smaller Curie temperature. Another term that could change with temperature is τ_0 because, considering the Néel-Brown model, it depends on the magnetic anisotropy.[46,63–65] These considerations indicate that our model could be further improved even considering strictly the S-W model.

V. CONCLUSIONS

We have evaluated the effect of the change of the magnetic anisotropy with the temperature on the phenomenology of the superparamagnetic and hysteresis properties of nanostructured materials. We have observed that some features of the superparamagnetism, which are commonly considered assuming that the magnetic anisotropy is constant with the temperature, are not fulfilled if the anisotropy varies. First, the relationship between the blocking temperature and the particle volume is not constant for different particle sizes. This can produce, as in the case of nickel, that nanoparticles with sizes up to the single-domain limit size are superparamagnetic at room temperature. Also, the analysis of the blocking temperature distribution of a material characterized by a particle-size distribution and realized considering a unique effective anisotropy constant gives rise to an apparent enhancement of the anisotropy. Second, the measurement time dependence of the blocking temperature does not follow the Arrhenius law and, in those cases where this law is accomplished, the calculated values of τ_0 and K_{ef} have no correlation with the real ones.

In the study of the temperature dependence of the coercivity, we have demonstrated that the law corresponding to the field dependence of the effective magnetic anisotropy varies if several anisotropy constants are considered in the description of the effective anisotropy. The main effect is the change of the exponential term ($\alpha<2$) that depends on the K_1 and K_2 values and that changes with the temperature due to the temperature dependence of these anisotropy constants. This produces that the temperature dependence of the coercive field does not follow the S-W power law or, in case it follows that power law, the obtained values of the coercive field at zero temperature and the β exponent depend on the K_1 and K_2 values and on the particle size. In particular, β can be larger than the 0.5 value expected with the S-W model. These results show the important effect of the temperature dependence of the intrinsic magnetic properties in the magnetic behavior of the nanostructured materials.

ACKNOWLEDGMENTS

The author thanks P. Mazzoldi, C. Sangregorio, C. Innocenti, D. Givord, and M. P. Morales for their fruitful discussions and comments to the text. This work was supported by the Italian National Research Project (PRIN).

*Electronic address: dejulian@padova.infm.it

[1] J. L. Dormann, D. Fiorani, and E. Tronc, Adv. Chem. Phys. **98**, 283 (1997).

[2] X. Batlle and A. Labarta, J. Phys. D **35**, R15 (2002).

[3] R. Skomski, J. Phys.: Condens. Matter **15**, R841 (2003).

[4] J. Bansmann, S. Baker, C. Binns, J. Blackman, J.-P. Bucher, J. Dorantes-Dávila, V. Dupuis, L. Favre, D. Kechrakos, A. Kleibert, K.-H. Meiwes-Broer, G. M. Pastor, A. Pérez, O. Toulem-

onde, K. N. Trohidou, J. Tuaillon, and Y. Xie, Surf. Sci. Rep. **56**, 189 (2005).
[5] B. Martínez, X. Obradors, L. Balcells, A. Rouanet, and C. Monty, Phys. Rev. Lett. **80**, 181 (1998).
[6] D. A. Garanin and H. Kachkachi, Phys. Rev. Lett. **90**, 065504 (2003).
[7] F. Luis, J. M. Torres, L. M. García, J. Bartolomé, J. Stankiewicz, F. Petroff, F. Fettar, J.-L. Maurice, and A. Vaurés, Phys. Rev. B **65**, 094409 (2002).
[8] E. C. Stoner and E. P. Wohlfarth, Philos. Trans. R. Soc. London, Ser. A **240**, 599 (1948).
[9] C. Kittel, Rev. Mod. Phys. **21**, 541 (1949).
[10] C. Bean and J. D. Livingston, J. Appl. Phys. **30**, 120S (1959).
[11] L. Néel, Ann. Geophys. (C.N.R.S.) **5**, 99 (1949).
[12] R. Street and J. C. Wooley, Proc. Phys. Soc., London, Sect. A **62**, 562 (1949).
[13] M. El-Hilo, K. O'Grady, and R. W. Chantrell, J. Magn. Magn. Mater. **117**, 21 (1992).
[14] R. Sappey, E. Vincent, N. Hadacek, F. Chaput, J. P. Boilot, and D. Zins, Phys. Rev. B **56**, 14551 (1997).
[15] W. Brown, Phys. Rev. **130**, 1677 (1963).
[16] U. Nowak and D. Hinzke, J. Appl. Phys. **85**, 4337 (1999).
[17] R. M. White, J. Magn. Magn. Mater. **226**, 2042 (2001).
[18] E. F. Kneller, J. Appl. Phys. **34**, 656 (1963).
[19] R. H. Victora, Phys. Rev. Lett. **63**, 457 (1989).
[20] W. Wernsdorfer, E. B. Orozco, K. Hasselbach, A. Benoit, B. Barbara, N. Demoncy, A. Loiseau, H. Pascard, and D. Mailly, Phys. Rev. Lett. **78**, 1791 (1997).
[21] F. C. Fonseca, G. F. Goya, R. F. Jardim, R. Muccillo, N. L. V. Carreño, E. Longo, and E. R. Leite, Phys. Rev. B **66**, 104406 (2002).
[22] E. Tronc, D. Fiorani, M. Nogués, A. Testa, F. Lucari, F. D'Orazio, J. Grenéche, W. Wernsdorfer, N. Galvez, C. Chanéac, D. Mailly, and J. P. Jolive, J. Magn. Magn. Mater. **262**, 6 (2003).
[23] E. Tronc, M. Nogués, C. Chanéac, F. Lucari, F. D'Orazio, J. Grenéche, J. Jolivet, D. Fiorani, and A. Testa, J. Magn. Magn. Mater. **272-276**, 143 (2004).
[24] C. de Julián Fernández, G. Mattei, C. Sangregorio, C. Battaglin, D. Gatteschi, and P. Mazzoldi, J. Magn. Magn. Mater. **272-276**, e1235 (2004).
[25] R. H. Kodama and A. E. Berkowitz, Phys. Rev. B **59**, 6321 (1999).
[26] E. Bonet, W. Wernsdorfer, B. Barbara, A. Benoit, D. Mailly, and A. Thiaville, J. Appl. Phys. **83**, 4188 (1999).
[27] W. Wernsdorfer, Adv. Chem. Phys. **118**, 99 (2001).
[28] C. Thirion, W. Wernsdorfer, M. Jamet, V. Dupuis, P. Mélinon, A. Pérez, and D. Mailly, J. Appl. Phys. **91**, 7062 (2002).
[29] M. Jamet, W. Wernsdorfer, C. Thirion, D. Mailly, V. Dupuis, P. Mélinon, and A. Pérez, Phys. Rev. Lett. **86**, 4676 (2001).
[30] M. Jamet, M. Nègrier, V. Dupuis, J. Tuaillon-Combes, P. Mélinon, A. Pérez, W. Wernsdorfer, B. Barbara, and B. Baguenard, J. Magn. Magn. Mater. **237**, 293, (2001).
[31] M. Jamet, W. Wernsdorfer, C. Thirion, V. Dupuis, P. Mélinon, A. Pérez, and D. Mailly, Phys. Rev. B **69**, 024401 (2004).
[32] I. Joffe and R. Heuberger, Philos. Mag. **314**, 1051 (1974).
[33] K. D. Durst and H. Kronmüller, J. Magn. Magn. Mater. **59**, 86 (1986).
[34] H. Kronmüller, K. D. Durst, and G. Martinek, J. Magn. Magn. Mater. **69**, 149 (1987).
[35] P. Escudier, Ph.D. thesis, Grenoble University, 1973.
[36] E. P. Wohlfarth, *Iron, Cobalt and Nickel* (North Holland Publishing, Amsterdam, 1980), pp. 1–70.
[37] Y. Barnier, R. Pauthenet, and G. Rimet, C. R. Acad. Sci., Paris 253, 2839 (1961).
[38] W. J. Carr Jr., J. Appl. Phys. **29**, 436 (1958).
[39] W. J. Carr Jr., in *Handbuch für Physick*, edited by H. P. J. Wijn (Spring-Verlag, Berlin, 1966), vol. 18/2, p. 322.
[40] S. Chikazumi, *Introduction to Ferromagnetism* (Oxford Sci. Publ., Oxford, 1997).
[41] J. M. Coey, Phys. Rev. Lett. **27**, 1140 (1971).
[42] M. P. Morales, S. Veintemillas Verdaguer, M. I. Montero, C. J. Serna, A. Roig, L. Casas, B. Martínez, and F. Sandiumenge, Chem. Mater. **11**, 3058 (1999).
[43] L. Néel, J. Phys. Radium **15**, 225 (1954).
[44] F. J. Himpsel, J. E. Ortega, G. J. Mankey, and R. F. Willis, Adv. Phys. **47**, 511 (1998).
[45] K. O'Grady and A. Bradbury, J. Magn. Magn. Mater. **39**, 91 (1983).
[46] J. L. Dormann, D. Fiorani, and E. Tronc, J. Magn. Magn. Mater. **202**, 251 (1999).
[47] C. Djurberg, P. Svedlindh, P. Nordblad, M. F. Hansen, F. Bødker, and S. Mørup, Phys. Rev. Lett. **79**, 5154 (1997).
[48] W. Kleemann, O. Petracic, C. Binek, G. N. Kakazei, Y. G. Pogorelov, J. B. Sousa, S. Cardoso, and P. P. Freitas, Phys. Rev. B **63**, 134423 (2001).
[49] P. Jönsson, M. Hansen, P. Svedlindh, and P. Nordblad, J. Magn. Magn. Mater. **226-230**, 1315 (2001).
[50] D. Bonacchi, A. Caneschi, D. Gatteschi, C. Sangregorio, R. Sessoli, and A. Falqui, J. Phys. Chem. Solids **65**, 719 (2004).
[51] E. Tronc, A. Ezzir, R. Cherkaoui, C. M. Chanéac, M. Nogués, H. Kachkachi, D. Fiorani, A. Testa, J. Grenéche, and J. Jolivet, J. Magn. Magn. Mater. **221**, 79 (2000).
[52] S. Mørup, J. Magn. Magn. Mater. **266**, 110 (2003).
[53] M. Ulrich, J. García-Otero, J. Rivas, and A. Bunde, Phys. Rev. B **67**, 024416 (2003).
[54] O. Cador, F. Grasset, H. Haneda, and J. Etourneau, J. Magn. Magn. Mater. **268**, 232 (2004).
[55] D. Bonacchi, C. Sangregorio, C. de Julián Fernández, and D. Gatteschi submitted.
[56] H. Pfeiffer, Phys. Status Solidi A **118**, 295 (1990).
[57] P. Vavassori, E. Angeli, D. Bisero, F. Spizzo, and F. Ronconi, Appl. Phys. Lett. **79**, 2225 (2001).
[58] H. Zijlstra, in *Ferromagnetic Materials*, edited by E. P. Wohlfarth (North Holland Publishing, Amsterdam, 1980), vol. 3, p. 55.
[59] E. F. Kneller, IEEE Trans. Magn. **27**, 3588 (1991).
[60] S. E. Tannenwald and R. Weber, Phys. Rev. **121**, 715 (1961).
[61] O. L. S. Lieu, G. C. Alexandrakis, and M. A. Huerta, Phys. Rev. B **16**, 476 (1977).
[62] A. Michels, J. Weissmüller, A. Wiedenmann, and J. G. Barker, J. Appl. Phys. **87**, 5953 (2000).
[63] A. Aharoni, Phys. Rev. **135**, A447 (1964).
[64] A. Aharoni, Phys. Rev. **177**, 793 (1969).
[65] W. T. Coffey, D. S. F. Crothers, Y. P. Kalmykov, E. S. Massawe, and J. T. Waldron, Phys. Rev. E **49**, 1869 (1994).